Effects of the bacterial algicide IRI-160AA on cellular morphology of harmful dinoflagellates

Kaytee L. Pokrzywinski[a,c], Charles L. Tilney[a,d], Shannon Modla[b], Jeffery L. Caplan[b], Jean Ross[b], Mark E. Warner[a] & Kathryn J. Coyne[a,1]

[a]College of Earth, Ocean, and Environment, University of Delaware, 700 Pilottown Road, Lewes, DE 19958, USA

[b]Biomaging Center, Delaware Biotechnology Institute, University of Delaware, 15 Innovation Way, Newark, DE 19711, USA

[c]Present address: Engineer Research and Development Center, U.S. Army Corps of Engineers, 3909 Halls Ferry Rd, Vicksburg, MS 39180

[d]Present address: FWC Fish & Wildlife Research Institute, St. Petersburg, FL 33701

Algicide impacts morphology in dinophyta

[3]Corresponding author, E-mail: kcoyne@udel.edu; tel.: +1 302 645 4236; fax: +1 302 645 4007, 700 Pilottown Rd. / Lewes, DE 19958

Abstract

The algicide, IRI-160AA, induces mortality in dinoflagellates but not other species of algae, suggesting that a shared characteristic or feature renders this class of phytoplankton vulnerable to the algicide. In contrast to other eukaryotic species, the genome of dinoflagellates is stabilized by high concentrations of divalent cations and transition metals and contains large amounts of DNA with unusual base modifications. These distinctions set dinoflagellates apart from other phytoplankton and suggest that the nucleus may be a dinoflagellate-specific target for IRI-160AA. In this study, morphological and ultrastructural changes in three dinoflagellate species, *Prorocentrum minimum*, *Karlodinium veneficum* and *Gyrodinium instriatum*, were evaluated after short-term exposure to IRI-160AA using super resolution structured illumination microscopy (SR-SIM) and transmission electron microscopy (TEM). Exposure to the algicide resulted in cytoplasmic membrane blebbing, differing chloroplast morphologies, nuclear expansion, and chromosome expulsion and/or destabilization. TEM analysis showed that chromosomes of algicide-treated *K. veneficum* appeared electron dense with fibrous protrusions. In algicide-treated *P. minimum* and *G. instriatum*, chromosome decompaction occurred, while for *P. minimum*, nuclear expulsion was also observed for several cells. Results of this investigation demonstrate that exposure to the algicide destabilizes dinoflagellate chromosomes, although it was not clear if the nucleus was the primary target of the algicide or if the observed effects on chromosomal structure were due to downstream impacts. In all cases, changes in cellular morphology and ultrastructure were observed within two hours, suggesting that the algicide may be an effective and rapid approach to mitigate dinoflagellate blooms.

Key words: dinoflagellate; chromosome decompaction; nucleus; cell cycle inhibition; algicide; morphology

1. Introduction

Bacteria are often seen in close association with harmful algal blooms (HABs) and may play an important role in regulating bloom dynamics (Kim et al., 1998; Mayali and Azam, 2004; Bidle and Falkowski, 2004; Liu et al., 2008a; Yoshinaga et al., 2010; Inaba et al., 2014) by enhancing growth (Fukami et al., 1997; Liu et al., 2008b) or through production of algicidal compounds (Sakata et al., 2011; Zheng et al., 2011; Pokrzywinski et al., 2012; Li et al., 2014). Bacteria with algicidal properties often have varying levels of specificity, effective against a single species or genus (e.g. Li et al., 2014) or with activity against a broad range of phytoplankton species (e.g. Lovejoy et al., 1998; Hare et al., 2005; Pokrzywinski et al., 2012). Algicides that are affective against a narrow group of HAB species likely target a common feature or characteristic shared by those species. An example would be the growth inhibitory effects of L-Lysine and L-Lysine-containing peptides on cyanobacteria (Takamura et al., 2004), which may be a consequence of the unusual makeup of cyanobacteria cell walls (Hoiczyk and Hansel, 2000).

Previous reports (Hare et al., 2005; Pokrzywinski et al., 2012; Tilney et al., 2014) characterized the algicidal activity of bacterium *Shewanella* sp. IRI-160, which killed a broad range of species from six families within the Dinophyta, while having no significant impact on other phytoplankton. The bacterium was found to secrete a low molecular weight, water-soluble compound, referred to as IRI-160AA (Pokrzywinski et al. 2012). A recent study by Pokrzywinski et al. (submitted) investigated biochemical impacts of the algicide. The algicide inhibited cell cycle progression in dinoflagellates, with increased intracellar and extracellular ROS production, as well as increased caspase-like (DEVDase) activity, suggesting a

71 biochemically mediated, non-necrotic cell death pathway. Tilney et al. (2014) evaluated the
72 algicide's impact on dinoflagellate physiology and observed species-specific impacts on
73 photobiology. Previous studies demonstrating growth inhibition in non-photosynthetic
74 dinoflagellates (Hare et al. 2005; Pokrzywinski et al. 2012), however, suggest that the
75 chloroplast is not the primary target of the algicide.

76 Dinoflagellates comprise a diverse group of species with varying morphological and
77 physiological features, (Spector 1984; Taylor 1987) and include representatives from trophic
78 levels ranging from strictly autotrophic to mixotrophic, parasitic, and predatory species. In
79 contrast to the large diversity in morphological and physiological characteristics, the unique
80 features of the dinoflagellate nucleus are fairly well conserved across the phylum (Spector 1984;
81 Taylor 1987) which comprises some of the largest eukaryotic genomes (Wisecaver and Hackett
82 2011). A large number of chromosomes, ranging from 24 to 220, are required to package the
83 substantial amount of genomic material (Wisecaver and Hackett 2011). The chromosomes are
84 unusual in that they remain permanently condensed throughout the life cycle (Bhaud et al. 2000)
85 and have a low quantity of histone or basic/histone-like proteins (HLPs), which, in other
86 eukaryotes, are required for neutralizing the negative charge in the sugar-phosphate backbone of
87 DNA. Instead, there is a high proportion of metal ions in the dinoflagellate nucleus, where the
88 ratio of metal to DNA base pair is 1:1 (Sigee and Kearns 1982). Studies by Sigee and Kearns
89 (1982) and Levi-Setti et al. (2008) suggest that divalent cations, particularly calcium and
90 magnesium, and transition metals are required to neutralize the negative charge of DNA and also
91 provide structure to the permanently condensed DNA without resulting in steric hindrance. In
92 addition to metal ions, dinoflagellate DNA also has a high proportion of 5-hydroxymethyluracil
93 (5HmU), replacing 12-70 % of thymine in their DNA (discussed in Williams and Place 2014).

This modification is unique among eukaryotes, and only rarely observed in prokaryotes (Spector 1984; Taylor 1987; Lin 2011). The unique chromosome packaging and DNA base modifications of dinoflagellates makes the nucleus an attractive target for dinoflagellate-specific algicides, either through direct interaction with the algicide or through secondary impacts.

Here, changes in cellular morphology of dinoflagellates were examined after short-term exposure to IRI-160AA, with emphasis on identifying algicide-induced changes to the nucleus. Changes in cellular morphology were initially evaluated in three dinoflagellate species, *Karlodinium veneficum*, *Prorocentrum minimum* and *Gyrodinium instriatum*, using super resolution structured illumination microscopy (SR-SIM). The ultrastructure of organelles of *K. veneficum* and *P. minimum* were then examined using transmission electron microscopy (TEM). Results of this descriptive study were consistent with the hypothesis that IRI-160AA induced destabilization of chromosome structure while also showing species-specific morphological changes in response to the algicide.

2. Materials and Methods

2.1 Phytoplankton culture maintenance

Experiments were conducted on *Prorocentrum minimum* (Culture Collection of Marine Phytoplankton strain CCMP2233, ncma.bigelow.org), *Karlodinium veneficum* (CCMP2396) and *Gyrodinium instriatum* (CCMP2935). Cultures were maintained in sterile *f*/2 medium (Guillard 1975) adjusted to a salinity of 20 and at 25 ºC with approximately 185 µmol photons m^{-2} s^{-1} on a 12:12 hr light:dark cycle. All experiments were conducted on batch cultures in logarithmic stage growth. None of the cultures were axenic.

118

119 *2.2 Algicide production*

120

121 The algicide, IRI-160AA, was prepared as described in Pokrzywinski et al. (2012) with
122 the following modifications. The optical density (OD) of *Shewanella* sp. IRI-160 culture in LM
123 medium was measured after 18 hours using a NanoDrop 2000c (ThermoFisher Scientific,
124 Waltham, MA, USA) at 600 nm wavelengths. For consistency between batches, 100 mL of
125 culture adjusted to an OD of 1.5 was added to 900 mL of LM medium. The *Shewanella* sp. IRI-
126 160 culture was incubated at 25 ºC on an orbital shaker at 100 rpm, until it again reached an OD
127 of 1.5. The culture was then centrifuged at 4,000 xg for 5 min using a Sorvall RC-5B superspeed
128 centrifuge (DuPont Instruments, Wilmington, DE, USA). The supernatant was removed and
129 cells were washed with *f*/2 medium. The culture was resuspended in 800 mL *f*/2 medium and
130 incubated for 1 week at 25 ºC. After 1 week the supernatant was harvested via centrifugation at
131 4,000 x g for 5 min. The cell-free supernatant was autoclaved at 121 ºC for 20 min and was
132 further purified by passing through a C18 HYPER SEP solid phase extraction column (Thermo
133 Scientific, Waltham, MA, USA) as described in Pokrzywinski et al. (2012). Briefly, the cell free
134 algicidal supernatant was loaded onto a C18 column, the aqueous pass-through was collected and
135 the partially-purified extract was added directly to cultures at 10 % final (*v*/*v*). Multiple batches
136 of the algicide were produced in this way and tested individually on *Karlodinium veneficum*. All
137 batches used in this study exceeded 75% algicidal activity and were combined for this study to
138 ensure consistency. Aliquots of the partially-purified algicidal extract were stored at -80 ºC long
139 term (greater than 1 month) or at 10 ºC for short-term use (< 3 weeks). Previous research by
140 Pokrzywinski et al. (2012) showed that the algicide was stable for at least three weeks at 4 ºC
141 and for greater than 1 year at -80 ºC. The *f*/2 media used in this study was also loaded onto a

142 C18 column, the aqueous pass-through collected and used at 10 % final (*v/v*) in algal cultures as
143 a corresponding control.
144
145 *2.3 Cellular morphology*
146
147 Short-term changes in cellular morphology of *P. minimum*, *K. veneficum* and *G.*
148 *instriatum* were examined using fluorescent staining with super-resolution structured
149 illumination microscopy (SR-SIM). Cells were harvested from treatment cultures (250 mL final
150 volume) at 15 min intervals for approximately 2 hrs after a 10 % (*v/v*) addition of IRI-160AA.
151 Control cultures received a 10 % (*v/v*) addition of f/2 medium and were harvested at the same
152 time points. At each time point, an aliquot of each culture was concentrated at 1,000 xg for 5
153 min. The supernatant was decanted and cells were resuspended in 1 μg mL^{-1} CellMask Orange
154 (Molecular Probes/Life Technologies, Grand Island, NY) in PBS for *P. minimum* and *K.*
155 *veneficum* and 1.875 μg mL^{-1} for *G. instriatum*. After staining with CellMask Orange, cells were
156 washed with PBS, recentrifuged and fixed in 2 % (final volume) paraformaldehyde for 20 min at
157 4 °C. Cells were then centrifuged and resuspended in 2 mL DAPI solution [2 μg/mL 4'6'-
158 diamidino-2-phenylidole (Molecular Probes/Life Technologies) in 50 mM NaCl, 50 mM Tris-
159 HCl pH 7.5] for 5 minutes in the dark. Cells were collected by centrifugation and stored in 100
160 μL 30 % glycerol in PBS at 4 °C in the dark prior to SR-SIM.
161 Images were captured by SR-SIM on a Zeiss ELYRA PS.1 super-resolution microscope
162 (Carl Zeiss, Oberkochen, Germany) with a Plan-Apochromat 63x/1.4 oil objective. Chlorophyll
163 autofluorescence was acquired with 4 % 642 nm laser and a 655 longpass filter. Chromosomes
164 labeled with DAPI were acquired with 15 % 405 nm laser excitation and a 420 – 480 nm
165 bandpass filter. Cell membranes labeled with CellMask Orange (Life Technologies) were

166 acquired with 0.7 % 561 nm laser power and a 570 – 620 bandpass filter. Z-stacks were taken
167 using 5 phase shifts and 3 rotations of the structured illumination pattern and a 0.091 µm z-
168 interval. Structured illumination reconstructions were conducted with default settings in the Zen
169 2011 (Carl Zeiss) processing software.
170
171 *2.4 Cellular Ultrastructure*
172
173 The ultrastructure of *P. minimum* and *K. veneficum* were examined using TEM. Images
174 of *G. instriatum* were not obtained due to the fragility of this species. A 10 % (*v*/*v*) final
175 concentration in 100 mL cultures of IRI-160AA or *f*/2 medium (control) was added to cultures in
176 logarithmic growth phase. After 1.5 hr (*K. veneficum*) or 1.75 hr (*P. minimum*) incubation, 40
177 mL of culture was concentrated by centrifugation at 1000 xg for 5 min using a swinging bucket
178 centrifuge. The supernatant was discarded and cells were resuspended in 1 mL of 1 % EM-grade
179 glutaraldehyde in PBS and incubated overnight at 4 °C. The algae were again pelleted, and the
180 supernatant was removed leaving the cells in a paste-like consistency. The cell pellet was
181 transferred to either 1.2 mm x 200 µm or 1.5 mm x 200 µm high pressure freezer carriers, frozen
182 with a Leica EMPact high pressure freezer (Leica Microsystems, Wetzlar, Germany) and freeze
183 substituted in either 2 % glutaraldehyde in acetone or 2 % osmium tetroxide, 1 % water in
184 acetone using a Leica AFS (Automated freeze substitution: Leica Microsystems). Samples were
185 freeze substituted at -85 °C for 118 hr before being warmed at a rate of 4 °C hr^{-1} for 15 hr and
186 held at -20 °C for 5 hr. Samples were then warmed at a rate of 5 °C hr^{-1} for 5 hr, held at 4 °C for
187 2 hr, and transferred to room temperature for an additional 2 hr. Samples were washed with
188 anhydrous acetone and infiltrated with EMBed-812 resin (Electron Microscopy Sciences,

Hatfield, PA). Samples were embedded in BEEM capsules (Electron Microscopy Sciences) and polymerized at 60 °C for 24 hr. Resin-embedded samples were sectioned on a Reichert-Jung Ultracut E ultramictrotome (Leica Microsystems), and ultrathin sections were collected onto formvar/carbon-coated 200 mesh copper grids and post-stained with 2 % alcoholic uranyl acetate and Reynolds' lead citrate. Samples were imaged with a Libra 120 transmission electron microscope (Carl Zeiss) at 120kV and images were acquired with a Gatan Ultrascan 1000 CCD (Gatan, Inc., Pleasanton, CA, USA).

3. Results

3.1 Cellular morphology

Substantial morphological changes were observed by SR-SIM in all algicide-treated dinoflagellates after short-term (2hr) exposure to the algicide (Fig. 1). A typical nucleus, chloroplast(s) and plasma membrane were observed in all control cells (Fig. 1A,C,E and Suppl. Fig. 1A, 2A, and 3A). For *Prorocentrum minimum*, nine cells were imaged after exposure to the algicide (representative cells shown in Fig. 1B and Suppl. Fig. 1B-C). In all images, the chloroplasts appeared granular and enlarged compared to the controls (Fig. 1A, Suppl. Fig. 1A). In addition, the DNA was expelled from several of the imaged cells treated with the algicide (Suppl. Fig. 1B), while the cell and theca appeared intact. At each time point after exposure, cells were observed with a low apparent quantity of DNA and lack of chromosomal structure, while some cells were anucleated (Suppl. Fig. 1C) with chromosomal DNA at the periphery of the cell (Fig. 1B) or outside of the cell (Suppl. Fig. 1B).

Fourteen cells were imaged for *K. veneficum* after exposure to the algicide (represented by Fig. 1D and Suppl. Fig. 2B-G). The cellular membrane of algicide-treated cells appeared intact at all time points for the 2 hr experiment. The lipophilic membrane stain, CellMask orange (shown in green for contrast) was taken up by *K. veneficum* in both control and treated cells, so that internal membranes were also stained (Fig. 1C-D; Suppl. Fig. 2A-G). Lipid stained structures within the chloroplasts of both controls and treatments may represent a pyramidal pyrenoid (PP) in this species (discussed in Garcés et al. 2006). After short-term (2 hrs) exposure with IRI-160AA, there was an apparent increase in chloroplast volumes in *K. veneficum* (Suppl. Fig. 2C,E,G). The nucleus appeared to remain intact but elongation of the nucleus was observed in some of the cells after exposure to the algicide (Suppl. Fig. 2D-G) and was more obvious at later time points. In addition, the nucleus and chloroplasts were translocated to the periphery of the cell, often appearing as a bulge in the cell membrane (Suppl. Fig. 2B,D,F,G). Blebs were observed on the surface of the cellular membrane and formed around organelles that had migrated to the periphery.

Seven cells were imaged for algicide-treated *G. instriatum* (represented by Fig. 1F, Suppl. Fig. 3B-C). Short-term exposure of *G. instriatum* to the algicide resulted in increased cell size compared to controls (Fig. 1E-F). The cellular membrane of this athecate species remained intact in all images acquired, with blebs visible on the surface of several cells (Suppl. Fig. 3B-C). The chloroplasts appeared granular and compacted but with an apparent increase in volume compared to the control in all micrographs. The observed increase in cell size may be due to noticeable nuclear expansion in several of the images (Fig. 1F, Suppl. Fig. 3B-C). Additionally, there was an apparent decompaction and/or fragmentation of the chromosomes, as seen in Fig. 1F. In contrast to *K. veneficum* and *P. minimum*, the DNA was ejected from the cell in only one

of the seven images obtained.

3.2 Cellular Ultrastructure

Significant ultrastructural changes were observed in TEM images of algicide-treated *P. minimum* (Fig. 2-3). Ten images were obtained for control cells. Chloroplasts were located in the periphery of the cell, beneath the thecal plate and in many cases included a compound intra-chloroplast pyrenoid (Fig. 2A). The nucleus was centrally located and contained condensed chromosomes with distinct banding patterns composed of fibrils and granules (Fig. 2B-C). Trichocysts (extrusomes), which were square in cross-section, were located just under the plasma membrane (Fig. 2A). Cells also contained fibrous vesicles in the anterior region of the cell near the flagellar apparatus (Fig. 2A and 3C). In algicide-treated cells of *P. minimum* (19 images total), there was increased vacuolization in the cytoplasm (Fig. 2D). The nucleoplasm appeared less granular than the control cells (Fig. 2E). The nuclear membrane had broken down in places and chromosomes appeared partially or wholly outside of the nucleus (Fig. 2E-F). The fibrils and granules of chromosomes became less apparent and the edges of chromosomes became less distinct, indicative of chromosome decompaction (Fig. 2D-F). Electron-dense aggregates, likely ribosomes, appeared in vacuoles (Fig. 2D). There were minimal observable changes in the ultrastructure of mitochondria (less apparent cristae) in algicide-treated cells compared to controls (Fig. 3B,E). Greater changes were observed in chloroplasts, mitochondria and fibrous vesicles of *P. minimum* cells exposed to IRI-160AA (Fig. 3D-F) compared to controls (Fig. 3A-C). Chloroplasts contained more inter-thylakoid electron dense regions in algicide-treated cells (Fig. 3D) compared to controls (Fig. 3A). Most noticeable were regions where the inter-thylakoid space of algicide-treated cells had expanded and contained electron depleted regions

(Fig. 3D). Mitochondria were slightly enlarged, circular and also contained electron depleted regions (Fig 3E). After IRI-160AA treatment, the fibrous vesicles no longer had an organized pattern and appeared to contain fewer fibers (Fig. 3F) compared to controls (Fig. 3C).

The ultrastructure of *K. veneficum* after algicide treatment was also examined using TEM (Fig. 4-5). Twelve images were obtained for *K. veneficum* control cells (represented by Fig. 4A-C). In each, the chloroplasts were located in the periphery of the cell, just under the plasma membrane and contained thylakoids in stacks of three (Fig. 5A), as typical of a plastid derived from a tertiary endosymbiotic event (Morden and Sherwood 2002). The pyramidal pyrenoid (PP) was located in the chloroplast and did not have thylakoids. The mitochondria were observed with tubular cristae (Fig. 4A and 5C). Vacuoles were distributed throughout the cytoplasm. Aggregates of electron-dense granules, likely ribosomes, were distributed throughout the cytoplasm. The nuclei of *K. veneficum* control cells were centrally located in the cell and had electron dense chromosomes with a characteristic banding pattern typical of dinoflagellate chromosomes, and contained regularly spaced fibrils and granules (Fig. 4A-C). In algicide-treated cells of *K. veneficum* (12 images total, Fig. 4D), amphiesmal and nuclear membrane blebbing were visible. The nucleus and chloroplasts were relocated to opposite ends of the cell, consistent with images obtained with SR-SIM. This may be due to the presence of a large vacuole that had filled the inter-organelle space in the cytoplasm. The chloroplasts and PP were more spherical compared to the controls, while thylakoids were unchanged (Fig. 4A,D and 5B). Electron-dense aggregates were also visible in treated cells (Fig. 4D). The arches of chromosomes appeared more fibrous in algicide-treated cells of *K. veneficum*, suggesting that the algicide may have an effect on processes occurring in the perichromosomal layer (Fig. 4E,F).

4. Discussion

The study presented here evaluated the effects of algicide IRI-160AA on morphology of three dinoflagellate species, *P. minimum*, *K. veneficum* and *G. instriatum*. In all cases, impacts on the nucleus were consistent with disruption of chromosome structure. Observed algicidal effects, however, were species-specific (Fig. 6). In algicide treated *K. veneficum* the chromosomes were apparent at all times but the nuclei were translocated to the periphery of the cell, at times forming a bulge in the cell membrane (Fig. 1D and Suppl. Fig. 2B-G). Chromosomes of algicide-treated cells also appeared to be elongated and fixed in an anaphase like state at later time points (Suppl. Fig. 2D-G) (Soyer-Gobillard et al. 1990) while the nuclei and chromosomes of control cells remained unchanged over the course of this study (2 hours). In contrast, algicide-treated cells of *G. instriatum* showed considerable nuclear expansion, with decompaction of the chromosomes so that they appeared to be "unraveling" (Fig. 1F). The nuclear membrane also disintegrated in some cells of *G. instriatum*, allowing the DNA of this species to fill the cytosolic space (Suppl. Fig. 3C). In *P. minimum*, the impacts of the algicide on the nucleus were more variable. Cells were observed with chromosomes translocated to the periphery of the cell (Fig. 1B) or ejected from the cell (Suppl. Fig. 1B), resulting in anucleated cells in some cases (Suppl. Fig. 1C).

Although TEM images for *G. instriatum* were not obtained, ultrastructural images of *K. veneficum* and *P. minimum* confirmed significant impacts to chromosomes in these algicide treated cultures. Dinoflagellates have liquid crystalline chromosomes (LCCs), which are composed of a highly condensed core and transcriptionally active DNA loops that decondense at

304 the periphery of the chromosome (Oakley and Dodge 1979; Cachon et al. 1989; Minsky et al.
305 1997; Oldenbourg et al. 1998; Livolant et al. 2006). In the absence of nucleosomes, these
306 peripheral transcriptional loops are maintained through the dense structure of the LCCs in the
307 core DNA (Chow et al. 2010). Although the ratio of DNA to HLP ratio is low in dinoflagellates,
308 HLPs are essential in these species to maintain the extrachromosomal loops for transcription by
309 actively straightening DNA in the periphery of chromosomes (Chan and Wong 2007). The
310 mechanism by which transcription occurs on these whorls remains largely unknown (Sigee,
311 1984, 1986; Soyer-Gobillard et al., 1990; Rizzo, 1991; discussed in Beauchemin et al. 2012).
312 TEM analysis of the nucleus in *K. veneficum* showed electron dense chromosomes with poorly
313 identifiable banding patterns (Fig. 4E,F). In addition, the edges of chromosomes appeared more
314 fibrous, suggesting that the impact of the algicide on the structural integrity of chromosomes
315 may be interfering with transcription (Sigee 1984, 1986; Soyer-Gobillard et al. 1990; Rizzo
316 1991). Electron micrographs of *P. minimum* also revealed abnormal nuclear morphologies,
317 including the decompaction and subsequent expulsion or "leakage" of chromosomes into the
318 cytosol (Fig. 2E-F), possibly at the site of nuclear pores (visible in the control Fig. 2A).
319 Expulsion may be driven by the mechanical force associated with chromosome decompaction, in
320 a manner similar to expulsion of viral DNA (Tzlil et al. 2003).
321 In all three species examined here, substantial changes to the chloroplasts were also
322 noted. Chloroplasts were relocated to the periphery of the cell after algicide treatment, possibly
323 as a result of increased vacuolization and nuclear expansion. Analysis of electron micrographs
324 of *P. minimum* and *K. veneficum* revealed changes in chloroplast shape, with plastids in algicide-
325 treated cells appearing more spherical than in controls. Similar changes in chloroplast structure
326 were noted in *Arabidopsis thaliana* after exposure to the plant stress hormone methyl jasminate

(Zhang and Xing 2008) and were attributed to ROS production. Likewise, Pokrzywinski et al. (submitted) showed that exposure to the algicide resulted in significant increases in both intra- and extracellular ROS production, measured at 3 hours and over a 24-hour period, respectively. In spite of the clear impact on dinoflagellate chromosomes and chloroplasts, however, it is unclear from this study which of these is the proximal target of the algicide or if changes in nuclear and/or chloroplast structures represent secondary, downstream impacts. Hare et al. (2005) and Pokrzywinski et al. (2012) examined algicidal impacts of IRI-160AA on a range of dinoflagellates including heterotrophs *Pfiesteria piscicida*, which acquires chloroplasts through kleptochlorplasty (Lewitus et al., 1999), and *Oxyrrhis marina*. These studies demonstrated no significant differences in growth inhibition between heterotrophic dinoflagellates and phototrophic species after exposure to *Shewanella* IRI-160 (Hare et al., 2005) or to the algicidal filtrate (Pokrzywinski et al., 2012), and suggest that impacts observed on chloroplasts in this investigation are likely secondary to those on the nucleus.

5. Conclusions

Exposure to the algicide IRI-160AA produced by marine bacterium *Shewanella* sp. IRI-160 resulted in significant morphological changes in dinoflagellates. Changes to the nucleus and chloroplasts were most apparent, but the proximal target of the algicide was not identified here. In all cases, changes in cellular morphology and ultrastructure were observed within two hours, suggesting that the algicide may be an effective approach to quickly mitigate dinoflagellate blooms. Future work should focus on isolation and characterization of the algicidal compound, IRI-160AA.

6. Acknowledgements

This work was supported by the National Oceanic and Atmospheric Association (NOAA) Prevention, Mitigation and Control of HABs (PCM HAB) program (Grant # NA10NOS4780136 to KJC and MEW, contribution number PCM034). This work was also made possible by the National Science Foundation EPSCoR Grant No. IIA-1301765 and the State of Delaware.

359 **References**

360

361 Beauchemin, M., Roy, S., Daoust, P., Dagenais-Bellefeuille, S., Bertomeu, T., Letourneau, L.,
362 Lang, B.F., Morse, D., 2012. Dinoflagellate tandem array gene transcripts are highly conserved
363 and not polycistronic. PNAS. 109(39): 15793-15798.

364

365 Bhaud, Y., Guillebault, D., Lennon, J., Defacque, H., Soyer-Gobillard, M.O., Moreau, H., 2000.
366 Morphology and behaviour of dinoflagellate chromosomes during the cell cycle and mitosis. J.
367 Cell. Sci. 113(7): 1231-1239.

368

369 Bidle, K.D., Falkowski, P.G., 2004. Cell death in planktonic, photosynthetic microorganisms.
370 Nat. Rev. Microbiol. 2(8): 643-655.

371

372 Cachon, J., Sato, H., Cachon, M., Sato, Y., 1989. Analysis by polarizing microscopy of
373 chromosomal structure among dinoflagellates and its phylogenetic involvement. Biol. Cell.
374 65:51–60.

375

376 Chan, Y.H., Wong, J.T.Y., 2007. Concentration-dependent organization of DNA by the
377 dinoflagellate histone-like protein HCc3. Nucleic Acids Res. 35:2573–2583

378

379 Chow, M.H., Yan, K.T., Bennett, M.J., Wong, J.T., 2010. Birefringence and DNA condensation
380 of liquid crystalline chromosomes. Eukaryotic Cell 9(10):1577-1587.

381 Fukami, K., Nishijima, T., Ishida, Y., 1997. Stimulative and inhibitory effects of bacteria on the
382 growth of microalgae. Hydrobiologia 358, 185-191.
383
384 Garcés, E., Fernandez, M., Penna, A., Van Lenning, K., Gutierrez, A., Camp, J., Zapata, M.,
385 2006. Characterization of NW Mediterranean *Karlodinium* spp. (Dinophyceae) strains using
386 morphological, molecular, chemical, and physiological methodologies. J. Phycol. 42: 1096-1112.
387 DOI: 10.1111/j.1529-8817.2006.00270.x
388
389 Guillard, R.R.L., 1975. Culture of Phytoplankton for Feeding Marine Invertebrates. In: Smith
390 WL, Chanley MH [Eds.], Culture of Marine Invertebrate Animals. Plenum Press, New York, pp.
391 26–60.
392
393 Hare, C.E., Demir, E.D., Coyne, K.J., Cary, S.C., Kirchmen, D.L., Hutchins, D., 2005. A
394 bacterium that inhibits the growth of *Pfiesteria piscicida* and other dinoflagellates. Harmful
395 Algae 4(2): 221-234.
396
397 Hoiczyk, E., Hansel, A., 2000. Cyanobacterial cell walls: news from an unusual prokaryotic
398 envelope. Journal of Bacteriology 182(5):1191-1199.
399
400 Inaba, N., Watanabe, T., Sakami, T., Nishi, H., Tahara, Y., Imai, I., 2014. Temporal and spatial
401 distribution of algicidal and growth-inhibiting bacteria in the coastal sea of southwest Japan. J
402 Plankton Res 36(2), 388-397.
403

404 Kim, M.C., Yoshinaga, I., Imai, I., Nagasaki, K., Itakura, S., Ishida, Y., 1998. A close
405 relationship between algicidal bacteria and termination of *Heterosigma akashiwo*
406 (Raphidophyceae) blooms in Hiroshima Bay, Japan. Mar Ecol-Prog Ser 170, 25-32.
407
408 Levi-Setti, R., Gavrilov, K.L., Rizzo, P.J., 2008. Divalent cation distribution in dinoflagellate
409 chromosomes imaged by high-resolution ion probe mass spectrometry. Eur. J. Cell. Bio. 87: 963-
410 976.
411
412 Lewitus, A.J., Glasgow, H.B., Burkholder, J.M., 1999. Kleptoplastidy in the toxic dinoflagellate
413 *Pfiesteria piscicida* (Dinophyceae). J Phycol 35(2), 303-312.
414
415 Li, Z.H., Lin, S.Q., Liu, X.L., Tan, J., Pan, J.L., Yang, H., 2014. A freshwater bacterial strain,
416 *Shewanella* sp Lzh-2, isolated from Lake Taihu and its two algicidal active substances,
417 hexahydropyrrolo[1,2-a]pyrazine-1,4-dione and 2, 3-indolinedione. Appl Microbiol Biot 98(10),
418 4737-4748.
419
420 Lin, S., 2011. Genomic understanding of dinoflagellates. Research in Microbiology 162: 551-
421 569.
422
423 Liu, J.Q., Lewitus, A.J., Kempton, J.W., Wilde, S.B., 2008a. The association of algicidal bacteria
424 and raphidophyte blooms in South Carolina brackish detention ponds. Harmful Algae 7(2): 184-
425 193.
426

427 Liu, J.Q., Lewitus, A.J., Brown, P., Wilde, S.B., 2008b. Growth-promoting effects of a
428 bacterium on raphidophytes and other phytoplankton. Harmful Algae 7(1): 1-10.
429
430 Livolant, F., Mangenot, S., Leforestier, A., Bertin, A., de Frutos, M., Raspaud, E., Durand, D.,
431 2006. Are liquid crystalline properties of nucleosomes involved in chromosome structure and
432 dynamics? Philos. Trans. R. Soc. Lond. A Math. Phys. Eng. Sci. 364: 2615–2633.
433
434 Lovejoy, C., Bowman, J.P., Hallegraeff, G.M., 1998. Algicidal effects of a novel marine
435 *Pseudoalteromonas* isolate (class Proteobacteria, gamma subdivision) on harmful algal bloom
436 species of the genera *Chattonella*, *Gymnodinium*, and *Heterosigma*. Appl Environ Microb 64(8),
437 2806-2813.
438
439 Mayali, X., Azam, F., 2004. Algicidal bacteria in the sea and their impact on algal
440 blooms. J. Eukaryot. Microbiol. 51(2): 139-144.
441
442 Minsky, A., Ghirlando, R., Reich, Z., 1997. Nucleosomes: a solution to crowded intracellular
443 environment? J. Theor. Biol. 188: 379–385.
444
445 Morden, C.W., Sherwood, A.R., 2002. Continued evolutionary surprises among dinoflagellates.
446 PNAS. 99(18): 11558-11560.
447
448 Oakley, B.R., Dodge, J.D., 1979. Evidence for a double-helically coiled toroidal chromonema in
449 the dinoflagellate chromosome. Chromosoma. 70: 277–291.

Oldenbourg, R., Salmon, E.D., Tran, P.T., 1998. Birefringence of single and bundled microtubules. Biophys. J. 74: 645–654.

Pokrzywinski, K.L., Place, A.R., Warner, M.E., Coyne, K.J., 2012. Investigation of the algicidal exudate produced by *Shewanella* sp. IRI-160 and its effect on dinoflagellates. Harmful Algae 19: 23-29.

Rizzo, P.J., 1991. The enigma of the dinoflagellate chromosome. J. Protozool. 38: 246-252.

Sakata, T., Yoshikawa, T., Nishitarumizu, S., 2011. Algicidal activity and identification of an algicidal substance produced by marine *Pseudomonas* sp. C55a-2. Fisheries Sci 77(3), 397-402.

Sigee, D.C., Kearns, L.P., 1982. X-ray microanalysis of unfixed chromatin in dinoflagellate cells prepared by a monolayer cryotechnique. J. Biochem. Biophys. Methods 6: 23-30.

Sigee, D.C., 1984. Structural DNA and genetically active DNA in dinoflagellate chromosomes. BioSystems 16: 203-210.

Sigee, D.C., 1986. The dinoflagellate chromosome. Advances in Botanical Research. 12: 205-264.

Skerratt, J.H., Bowman, J.P., Hallegraeff, G., James, S., Nichols, P.D., 2002. Algicidal bacteria

473 associated with blooms of a toxic dinoflagellate in a temperate Australian estuary. Mar. Ecol.
474 Prog. Ser. 244: 1-15.
475
476 Soyer-Gobillard, M.O., Géraud, M.L., Coulaud, D., Barray, M., Théveny, B., Révet, B., Delain,
477 E., 1990. Location of B- and Z-DNA in the chromosome of a primitive eukaryote dinoflagellate.
478 J. Cell. Biol. 111: 293-308.
479
480 Spector, D.L., 1984. Dinoflagellate nuclei. In D. L. Spector [ed.]: Dinoflagellates. Academic
481 Press, Inc., Orlando, FL, USA, pp. 107-147.
482
483 Takamura, Y., Yamada, T., Kimoto, A., Kanehama, N., Tanaka, T., Nakadaira, S., Yagi, O.,
484 2004. Growth inhibition of *Microcystis* cyanobacteria by L-lysine and disappearance of natural
485 *Microcystis* blooms with spraying. Microbes and Environments, 19(1), 31-39.
486
487 Taylor, F.J.R., 1987. The Biology of Dinoflagellates. Wiley, Johns & Sons, Inc. Hoboken, NJ,
488 USA.
489
490 Tilney, C.L., Pokrzywinski, K.L., Coyne, K.J., Warner, M.E., 2014. Growth, death and
491 photobiology of dinoflagellates (Dinophyceae) under bacterial-algicide control. J. Appl. Phycol.
492 26: 2117-2127. DOI 10.1007/s10811-014-0248-z
493
494 Tzlil, S., Kindt, J.T., Gelbart, W.M., Ben-Shaul, A., 2003. Forces and pressures in DNA
495 packaging and release from viral capsids. Biophys. J. 84:1616–1627.

Williams, E.P. and Place, A.R. (2014). The role of 5-hydroxymethyl uracil in the evolution of the dinokaryon.Kim, H.G., B. Reguera, G. Hallegraeff, C.K. Lee, M.S. Han and J.K Choi (eds). Harmful Algae 2012, Proceedings of the 15th International Conference on Harmful Algae. International Society for the Study of Harmful Algae 2014, Copenhagen, ISBN 978-87-990827-4-2. pp 153-156.

Wisecaver, J.H., Hackett, J.D. 2011. Dinoflagellate genome evolution. Annu. Rev. Microbiol. 65: 369-387.

Yoshinaga, I., Park, J.H., Nishikawa, T., Imai, I., 2010. Algicidal bacteria in particle-associated form and in free-living form during a diatom bloom in the Seto Inland Sea, Japan. Aquat Microb Ecol 60(2), 151-161.

Zhang, L., Xing, D., 2008. Methyl jasmonate induces production of reactive oxygen species and alterations in mitochondrial dynamics that precede photosynthetic dysfunction and subsequent cell death. Plant Cell. Physiol. 49: 1092-1111.

Zheng, T.L.L., Bai, S.J.J., Huang, L.P.P., Su, J.Q.Q., Tian, Y., 2011. Algicidal effects of a novel marine actinomycete on the toxic dinoflagellate *Alexandrium tamarense*. Curr Microbiol 62(6), 1774-1781.

520 **Figure Legends:**

521

522 **Fig. 1**: Super resolution images of dinoflagellate cellular morphologies after short-term exposure
523 to 10 % (*v*/*v*) IRI-160AA. Control cells (left panel) and algicide-treated cells (right panel) for
524 *Prorocentrum minimum* (A and B), *Karlodinium veneficum* (C and D) and *Gyrodinium*
525 *instriatum* (E and F). Cells were stained with the nuclear dye DAPI and membrane dye Cell
526 Mask Orange (shown in green for contrast).

527

528 **Fig. 2:** Electron micrographs of *Prorocentrum minimum*. Cellular (A, C) and chromosome (B,
529 D) ultrastructure after exposure to IRI-160AA (C-D) are shown with respective controls for
530 comparison (A-B). N = nucleus, Ch = chloroplast, Py = pyrenoid, S = starch, M = mitochondria,
531 CB= cajal body, Th = theca, V = vacuole, ER = endoplasmic reticulum, T = trichocyst, R =
532 ribosome aggregate, G = golgi, FV = fibrous vesicles and Cr = chromosome. Scale bar is 1μm in
533 panels A and D and 0.2 μm in panels B, C, E and F. Arrows in B indicate fibrils and granules.
534 The arrow in D indicates loss of chromosomal structure and partial expulsion from the nucleus.

535

536 **Fig. 3:** Electron micrographs of *Prorocentrum minimum* chloroplast (A, D), mitochondria (B, E)
537 and fibrous vesicles (C, F) after treatment with IRI-160AA (D, E, F) with respective controls for
538 comparison (A, B, C). Scale bar is 0.2 μm.

539

540 **Fig. 4:** Electron micrographs of *Karlodinium veneficum*. Cellular (A, D) and chromosome (B-C,
541 E-F) ultrastructure for IRI-160AA-treated cells (D-F) are shown with respective controls for
542 comparison (A-C). N = nucleus, Ch = chloroplast, S = starch, M = mitochondria, V = vacuole,

PP = pyramidal pyrenoid, Th = theca, Am = amphiesmal, CB = cajal body, R = ribosome aggregate, T = trichocyst, Bl = bleb and Cr = chromosome. Scale bar is 1 μm in A and D and 0.2 μm in B and E. C and F are magnifications of panels B and E, respectively. Arrows in C indicate fibrils and granules. Arrow in F indicates fibrous protrusions in the perichromosomal space.

Fig. 5: Electron micrographs of *Karlodinium veneficum* chloroplast (A-B) and mitochondria (C-D) ultrastructure after exposure to IRI-160AA (B, D) with respective controls for comparison (A, C). Scale bar is 1 μm in panels A and B and 0.5 μm in panels C and D.

Fig. 6: Super resolution images of characteristic chromosome/nuclear morphologies in dinoflagellates. Nuclear morphologies for *Prorocentrum minimum* (A-B), *Karlodinium veneficum* (C-D) and *Gyrodinium instriatum* (E-F) after exposure to 10 % (*v/v*) IRI-160AA (B, D, F) with respective controls for comparison (A, C, E). Scale bars are 50 μm (A-C, E), 33 μm (D) or 100 μm (F).

Prorocentrum minimum

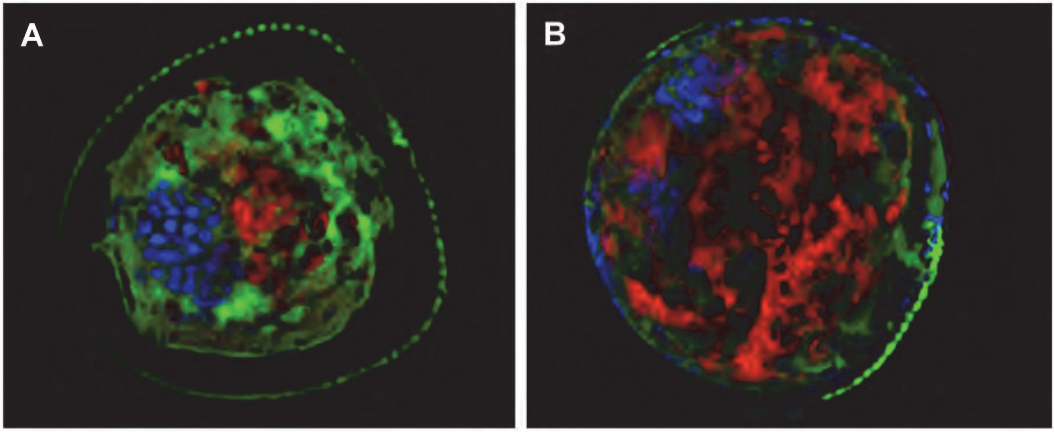

Karlodinium veneficum

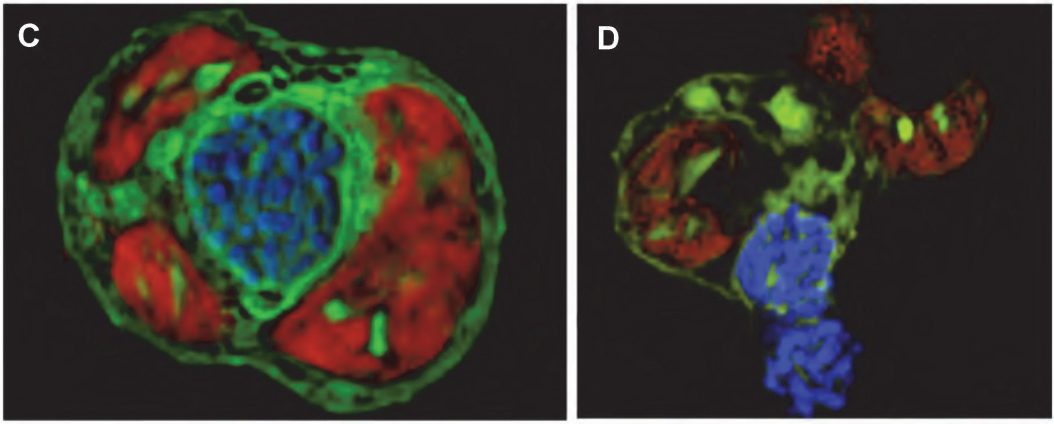

Gyrodinium instriatum

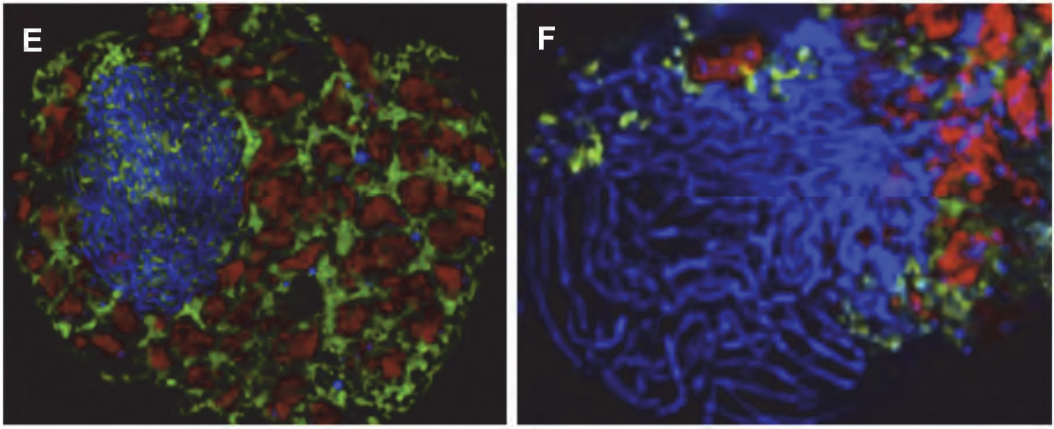

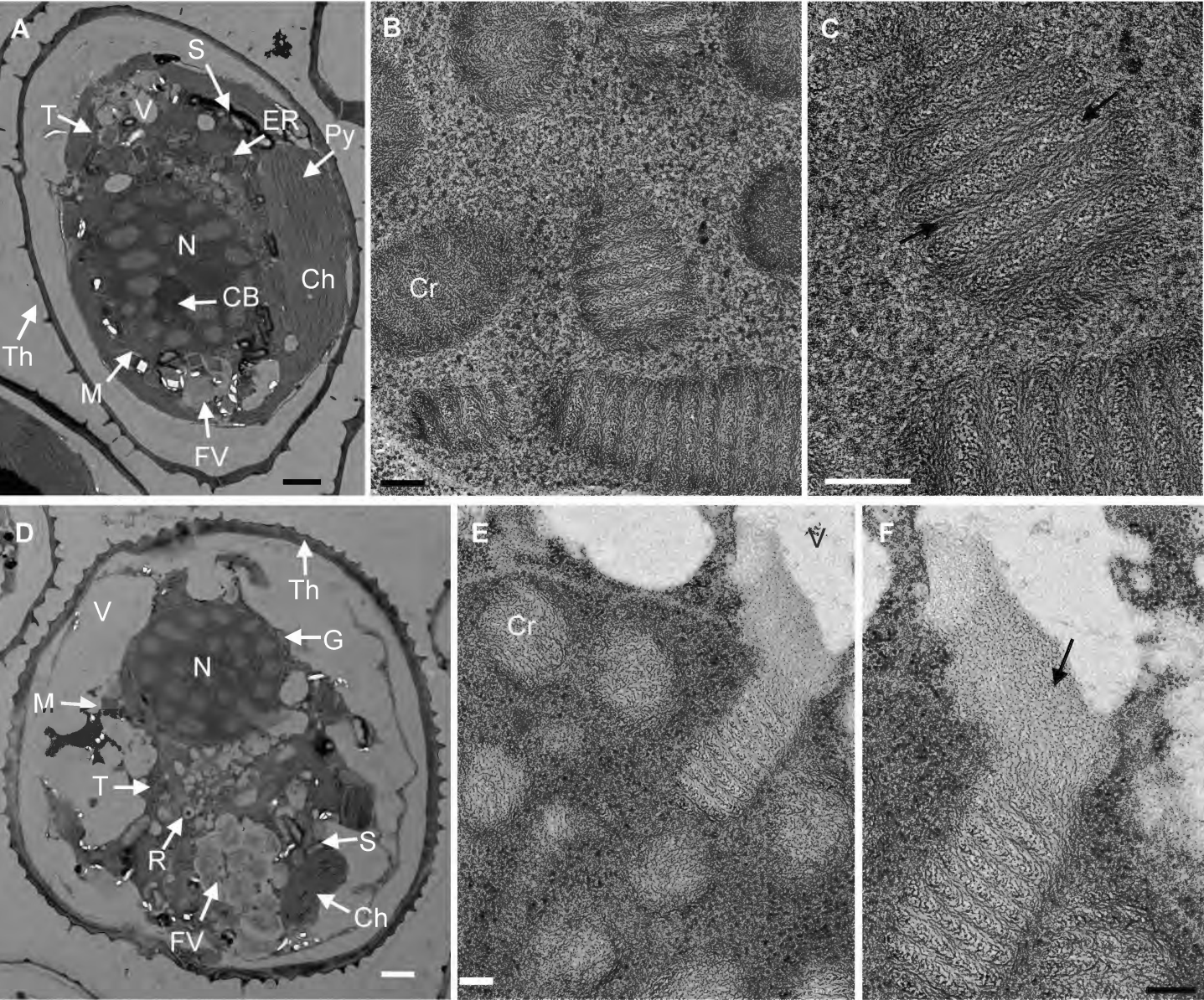
A
S
T
V
ER
Py
N
Ch
CB
Th
M
FV
B
Cr
C
D
Th
V
G
N
M
T
R
S
FV
Ch
E
V
Cr
F

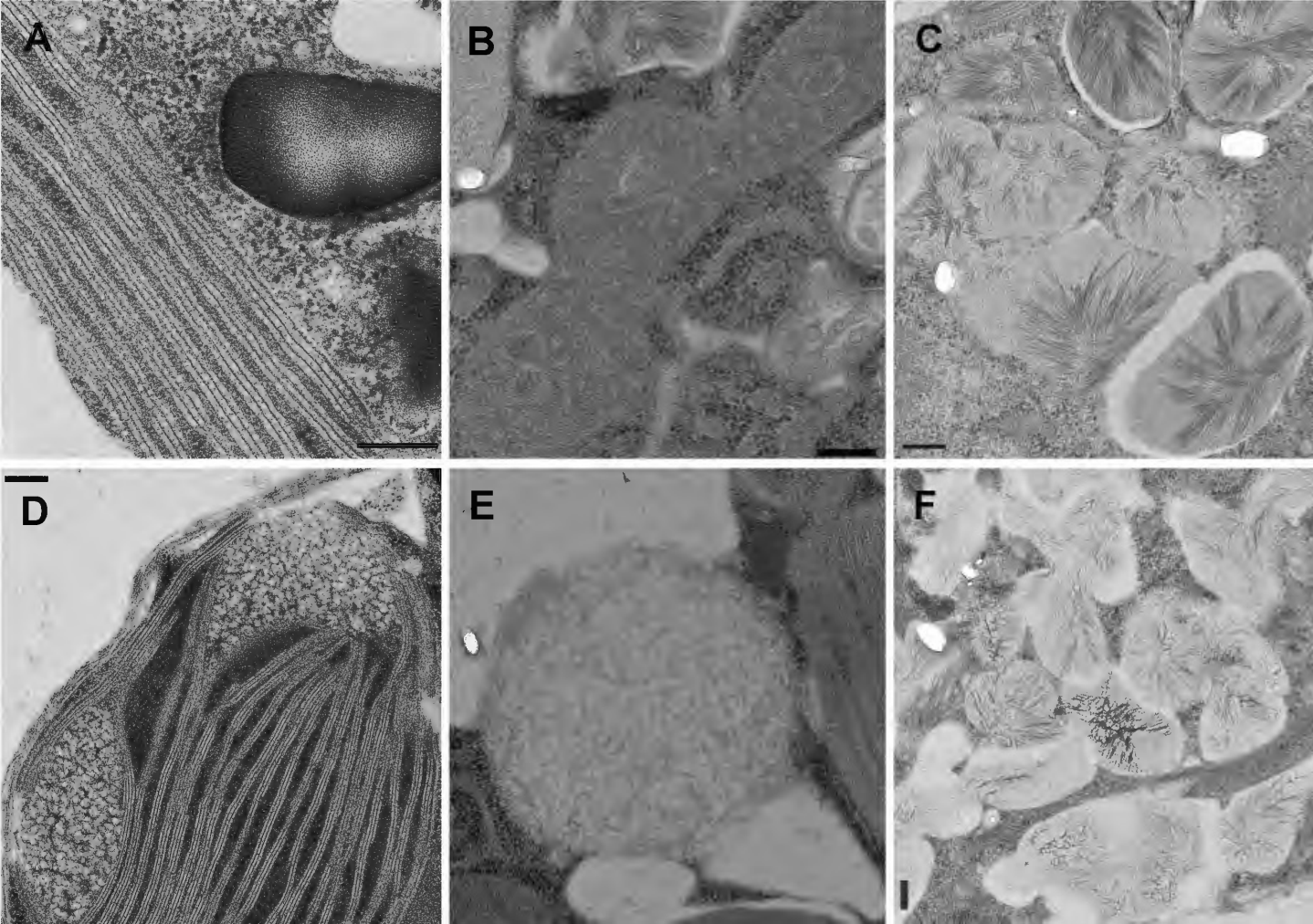
A
B
C
D
E
F

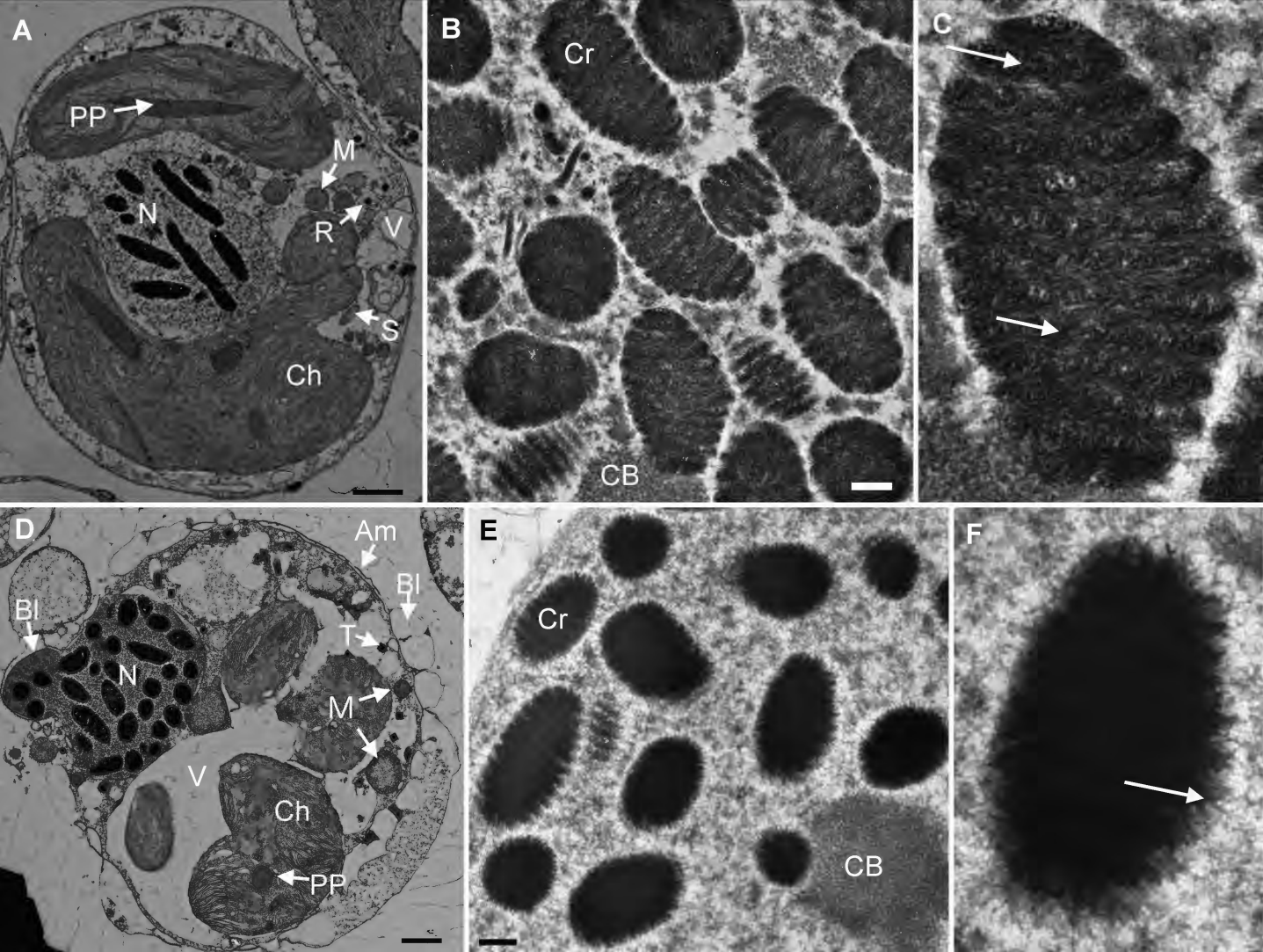
A
PP
M
N
R
V
S
Ch
B
Cr
CB
C
D
Am
Bl
Bl
T
N
M
V
Ch
PP
E
Cr
CB
F

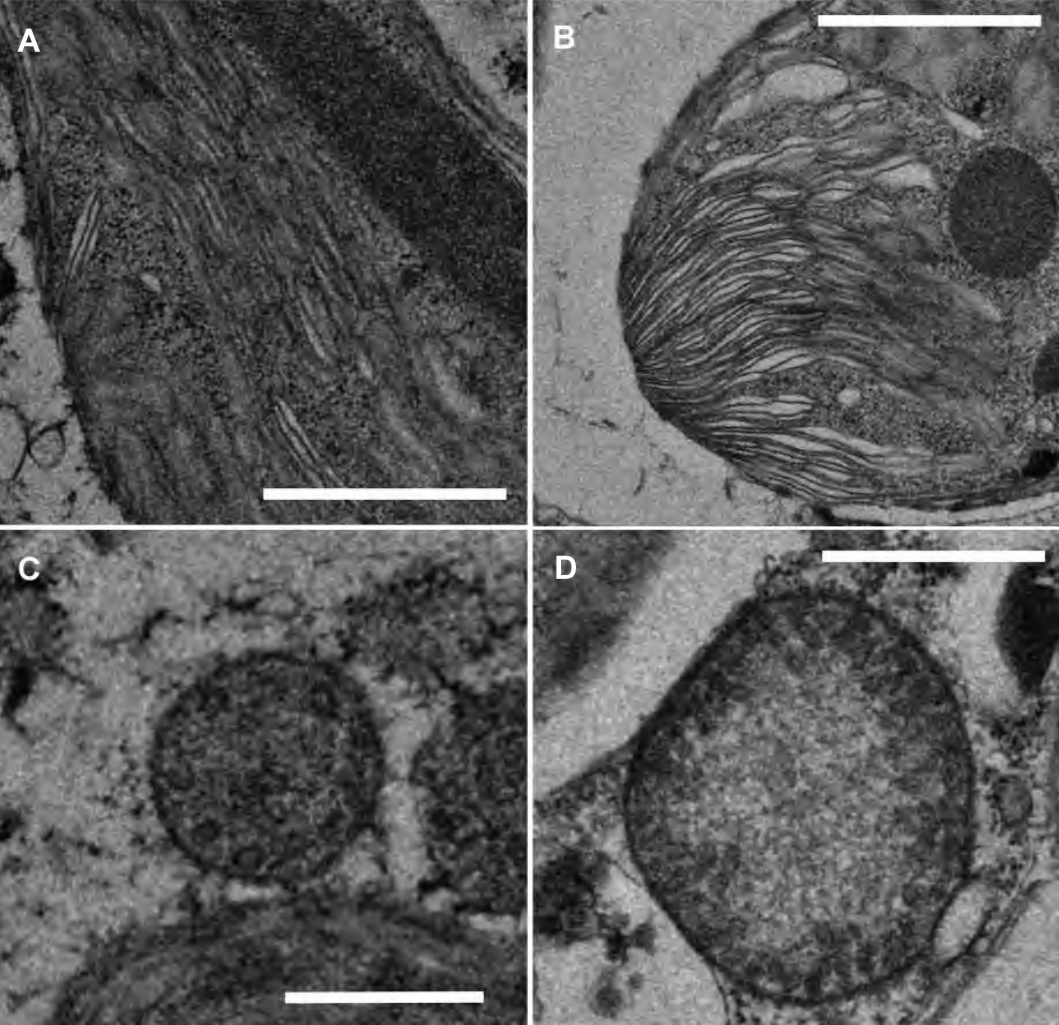
A
B
C
D

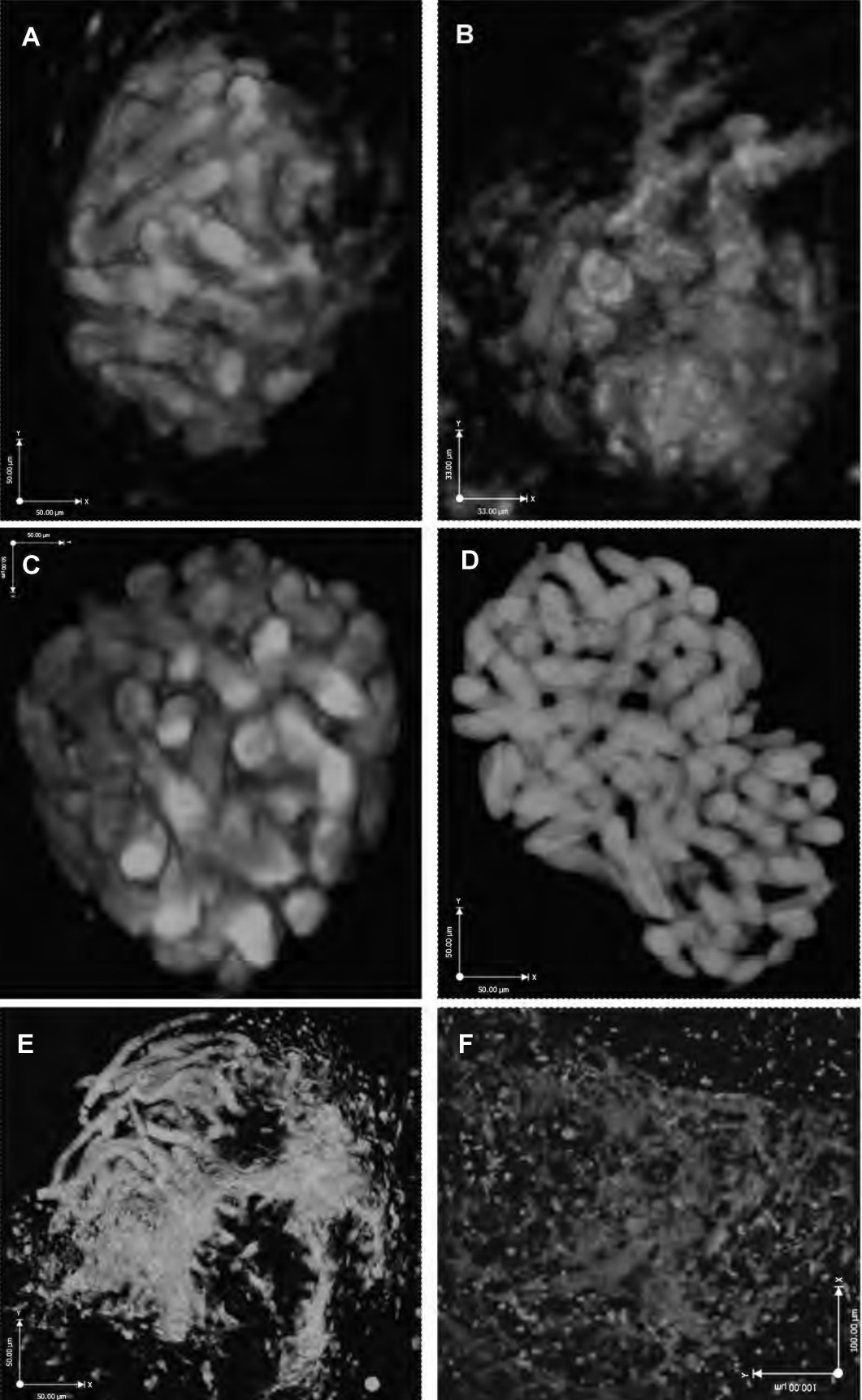
A
B
C
D
E
F
50.00 µm
33.00 µm
100.00 µm